Comparison of magnetic fields and Doppler velocities in an X-class solar flare as measured by D1, D2, D3, H-alpha and NiI 5892.9 lines

Article *in* Advances in Space Research · August 2024

DOI: 10.1016/j.asr.2024.08.006

3 authors, including:

Vsevolod G. Lozitsky
Taras Shevchenko National University of Kyiv
177 PUBLICATIONS **673** CITATIONS
SEE PROFILE

Ivan I Yakovkin
Taras Shevchenko National University of Kyiv
41 PUBLICATIONS **69** CITATIONS
SEE PROFILE

Comparison of magnetic fields and Doppler velocities in an X-class solar flare as measured by D1, D2, D3, Hα, and NiI 5892.9 lines

V.G. Lozitsky*, I.I. Yakovkin, N.I. Lozitska

Astronomical Observatory of the Taras Shevchenko National University of Kyiv, Observatorna St. 3, Kyiv 04053, Ukraine

Received April 4, 2024; Accepted 3 Aug 2024

Abstract

The main goal of our research is to estimate the upper magnetic field limit in a flare using direct observations in spectral lines formed in a wide range of heights – from the photosphere to the transition region between the chromosphere and corona. Our method is based on the Stokes *V* spectro-polarimetry of D1, D2, D3, Hα, and NiI 5892.9 lines and the nearest spectral continuum, with a total spectral range of approximately 50 Å. The object of the study is the solar flare on 17 July 2004 (X1.1/2N class), which is associated with the active region NOAA 10649. The main results of our study are the following: (*a*) the maximum magnetic field strengths in the flare, measured directly from the splitting of the line profiles, reached 4.7–6.0 kG in the D1 and D2 lines, 1.9 kG in the D3 line, and only 0.6 kG in the H-alpha and Ni I lines; (*b*) Doppler (longitudinal) velocities changed sign with height in the atmosphere, ranging from –4.5 to 7.7 km/s; (*c*) observational indications of stronger magnetic fields (> 6 kG) were not found when studying wide spectral intervals (up to 15 Å) around the Hα and D3 lines. On the basis of these results, it can be concluded that the studied solar flare had a significant altitudinal heterogeneity of the magnetic field and Doppler velocities, and the peak values of the magnetic field in the chromosphere (6 kG) surpassed those in the nearest sunspots at the photospheric level (2.8 kG). This likely indicates a local strengthening ("collapse") of the magnetic field in the region of the solar flare. The latter is confirmed by the fact that the Doppler velocities in the chromosphere had the opposite signs, facilitating increased local concentration of matter and magnetic field.

Keywords: Sun, solar flares, magnetic fields, spectro-polarimetry in D1, D2, D3, and Hα lines, super-strong fields.

1. Introduction

The upper magnetic field strength limit in the solar atmosphere currently remains undetermined. Until recently, it was believed that the strongest magnetic fields originate in sunspots, where, according to direct observations, the field strength is generally 2100–2900 G, occasionally reaching 3500–4000 G (Solanki, 2003; Pevtsov et al., 2014; Lozitska et al., 2015). Rare cases were recorded when the magnetic field reached 5.5–8.2 kG in sunspots (see, e.g., Livingston et al., 2006; Durán et al., 2020; Lozitsky et al., 2022).

*Corresponding author. Address: Astronomical Observatory of Taras Shevchenko National University of Kyiv, 3, Observatorna str., Kyiv 04053, Ukraine.
Tel.: +380 44 486 0906; fax: +380 44 481 4478.
E-mail addresses: vsevolod.lozitsky@knu.ua (Lozitsky V.G.), yakovkinii@gmail.com (Yakovkin I.I.) nloz@knu.ua (Lozitska N.I.).

Solar flares are very interesting and volatile processes in solar active regions, and could also contain the strongest fields. Each flare is a grandiose explosion in a wide range of heights in the solar atmosphere, with sharp increase in temperature, gas pressure and ionization of plasma. Hot flare plasma outside the magnetic flux tubes provides increased pressure on walls of these tubes, and may therefore increase the magnetic strength inside tubes. Additionally, an increase in plasma ionization leads to amplification of electric currents and magnetic fields, provided that the structure of magnetic field is force-free (Parker, 2001; Priest, 2014).

Unfortunately, magnetic field measurements in flares are more complex compared to sunspots. First, solar flares occur suddenly and develop rapidly. The most interesting phases of a flare can be missed if observations are carried out in a non-continuous regime. Such non-continuous regime is typical for spectro-polarimetric observations and is most suitable for magnetic field measurements in flares. Regarding the instruments working in the automatic regime such as SOHO/MDI filter magnetograph (Scherrer et al., 1995), these give mainly the longitudinal magnetic field component – not the magnetic field magnitude. In addition, in the case of the most powerful flares, practically all spectral lines have a relatively strong flare emission. In some cases, such an emission can distort the magnetographic signal, leading to incorrect measured field values and even polarities (Lozitskaya and Lozitskii, 1982).

Currently, there are very different estimates of local magnetic fields in solar flares – from 10^2 to 10^5 G (see, e.g., Harvey, 2012; Kleint, 2017; Libbrecht et al., 2019; Yakovkin and Lozitsky, 2022; 2023). As for the stronger magnetic fields in the specified range, due to methodological reasons the latter cannot be detected from spectropolarimetric measurements in a narrow spectral range, such as ± 1Å. After all, magnetic fields of $B \sim 10^5$ G can result in a Zeeman splitting of several angstroms. Lozitska et al. (2024) observed possible spectral manifestations of such fields at up to 10 Å from the primary emission in the line. For some instruments based on Fabry-Perot filters, such a wide spectral interval can be unachievable. It is well known that the dispersion region of the Fabry-Perot filter is narrower, the higher the spectral resolution of the instrument. For example, the 4.2-meter European telescope (Quintero Noda et al., 2022) has the dispersion area of the integral field spectropolarimeters spanning the range of at least 1 nm = 10 Å, i.e. it should be sufficient for such studies. However, it should be taken into account that near the boundary of the dispersion region, the quality of the spectrum image deteriorates quickly and the observation errors increase accordingly.

The best-suited tool for detecting and studying such extremely strong magnetic fields is likely a classical Echelle spectrograph. In the latter, the region of undistorted dispersion reaches thousands of angstroms. In addition, different diffraction orders are spatially separated, that is, they do not overlap in the focal plane of the spectrograph, where the focused spectrum is formed. In this respect, an Echelle spectrograph is superior to a conventional non-Echelle spectrograph, in which different diffraction orders are isolated by the application of appropriate spectral filters, rather than being spatially separated by a prism or other diffraction grating with a perpendicular dispersion direction. The mentioned spectral filters do not always guarantee a complete extinction of light from close orders, and therefore can produce weak artifacts due to contamination from different diffraction orders. It is worth mentioning that the largest solar telescope of its time LEST – a Large International Solar Telescope for the 1990's – was planned with a powerful Echelle spectrograph (Stenflo, 1985).

Taking into account the results of previous studies on extremely strong magnetic fields, published in Yakovkin and Lozitsky (2023), Lozitska et al. (2024), in the presented paper we try to find analogies to the corresponding spectral effects in the new observational material, which corresponds to the X-class solar flare. Since we cannot know in advance at which heights in the atmosphere and in which spectral regions these diagnostic effects may appear, we simultaneously analyze multiple spectral lines in a wide spectral interval of up to 50 Å, with line formation heights spanning approximately 2 Mm (Vernazza et al, 1981).

2. Observations and data processing

In the present study, we investigate the solar flare on 17 July 2004 of the X1.1/2N class, which occured in the active region NOAA 10649. This relatively small active region has been very flare-active, notably producing six X-class flares from July 15 to July 17, 2004, including X2 and X3 flares that occurred on July 15 and 16, respectively (https://spaceweather.com/). The magnetic type of this region was βγδ. The flare occurred in the tail part of the specified active region, close to the sunspot of negative, N, magnetic polarity with the magnetic strength of 2800 G and the heliocentric distance $\mu = 0.88$.

Observations of the flare were carried out by Vsevolod Lozitsky with the Echelle spectrograph of the Kyiv University Astronomical Observatory. From 8:01 to 8:16 UT, six Echelle Zeeman spectrograms of the flare were obtained with a circular polarization analyzer using ORWO WP3 photoemulsion. In this study, only the second spectrogram is analyzed. It was made with an exposure of 20s starting at 08:02 UT, about 6 minutes after of the X ray peak (7:56 UT) according to GOES data. At the moments 8:01 and 08:02 UT, the spectrum of the flare had bright emissions in Hα and D3, as well as less pronounced emissions in the D1 and D2 lines (Fig. 1). In order to explicitly refer to different locations in the investigated flare, below we introduce the lateral coordinate L, which in Fig. 1 increases from top to bottom.

The optical scheme of the telescope and some instrumental details were described by Lozitsky (2016). The Echelle spectrograph is a cross-dispersion instrument. Its optical design simultaneously employs a diffraction grating with profiled grooves to intensify light concentration, as well as a glass prism for dispersing diffraction orders. Therefore, the overlay of diffraction orders is entirely prevented, specifically due to the glass prism dispersing these orders to an appropriate degree. This is especially important for searching for subtle spectral effects far from the spectral line, in the spectral continuum region. In addition, the value of observations with the Echelle spectrograph is that a wide spectrum interval, from 3800 to 6600 Å, can be recorded simultaneously where many thousands of spectral lines can be observed.

Another advantage of such observations is that $I + V$ and $I - V$ spectra were obtained simultaneously, on separate adjacent bands of the spectrograms. This was achieved by using the circular polarization analyzer which consisted of a λ/4 plate in front of the entrance slit of the spectrograph and a beam splitting prism (analogous to the Wollaston prism) behind the entrance slit. Therefore, $I + V$ and $I - V$ spectra relate to the same moment of time and to the same locations on the Sun.

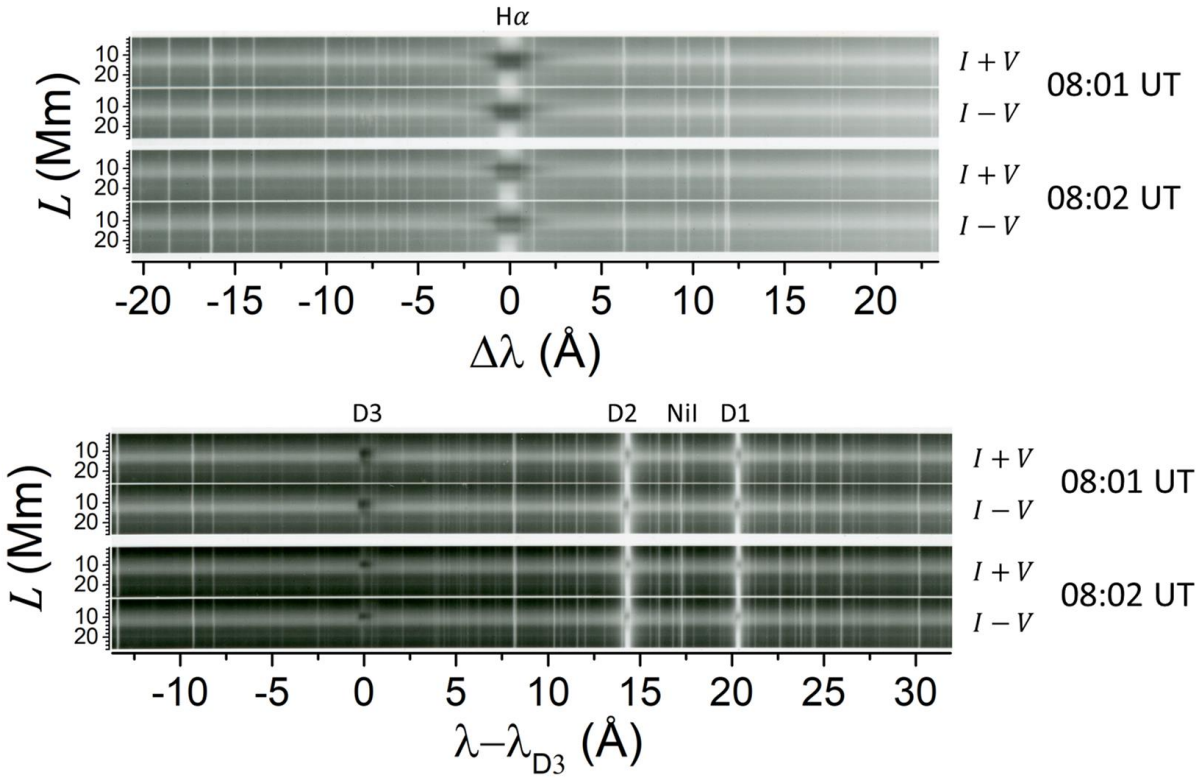

Figure 1. Fragments of the spectrum of the solar flare of 17 July 2004 at 08:01 and 08:02 UT, which contain the investigated spectral lines.

The Hα line was observed in the 31st order of diffraction, and D3 line – in in the 35th order. For the D3 line, the total length of the spectrum, which is simultaneously registered near this line, is 160 Å in the range from –112 Å to +48 Å relative to the center of the D3 line. Dispersion in this order is 770 mÅ per mm, and the FWHM of the instrumental profile is about 50 mÅ. For ORWO WP3 photographic plates, signal-to-noise ratio is about 100 when optimally exposed. The length of the entrance slit of the spectrograph was 2.2 mm, and its width was 0.06 mm, which corresponds to about 33 and 0.9 arc sec, respectively. However, due to image vibration, the actual spatial resolution of our observations is ≈ 1.5 Mm.

In order to obtain quantitative information on intensity distribution in spectra of the flare, the 08:02 UT spectrogram was scanned using the Epson Perfection V 550 scanner. To convert the scanned image intensity, it is necessary take into account the characteristic curve of the photographic material as well as the curve of the scanner itself. Both curves are nonlinear and require preliminary determination by special methods. In order to do this, we used a step attenuator, for which transmittances are precisely known. When converting photometrical densities into intensities, the scattered light in the spectrograph was taken into account by subtracting the intensities corresponding to the intervals between images of different diffraction orders of the spectrum of the Echelle spectrograph. Additional details on data processing of the Echelle Zeeman spectrograms were discussed in Yakovkin and Lozitsky (2022).

3. Results

3.1. *Selected spectral lines and their I ± V profiles*

Table 1 lists the selected spectral lines. In this Table, λ is the wavelength in angstroms (Å), *EP* is the excitation potential of the lower term in electron-volts (eV), W_{ekv} is the equivalent line width in milliangstroms (mÅ) in the spectrum of the quiet Sun (Moore et al., 1966), $g_{eff,LS}$ is the effective Lande factor for the case of spin-orbital (*LS*) interaction in an atom, $g_{eff,,PB}$ is the effective Lande factor with corrections for the Paschen – Back effect.

From experimental works by Banasek et al. (2003) and Hori et al. (1982) it follows that the Paschen-Back effect in the D1 and D2 lines occurs even at sub-kilogauss magnetic fields. This was verified by us on the basis of a comparison of the magnetic field strengths measured by the lines No. 1, 2 and 4 in the sunspot on July 24, 2023. If we use the theoretical Lande factors for the *LS* coupling to calibrate the splitting of the indicated lines, then an unrealistic picture occurs: the strongest magnetic field is measured in the chromospheric D2 line (No. 2), the intermediate magnetic field is indicated by the photospheric Ni I line (No. 4), and the weakest magnetic field – by the D1 line (No. 1). However, if we use the Lande factors $g_{eff,PB}$ corrected for the Paschen-Back effect for the lines No. 1 and 2, then the situation becomes quite realistic: photospheric line No. 4 shows a stronger magnetic field in the sunspot than chromospheric lines No. 1 and 2 in all locations. That is why the results presented below for the D1 and D2 lines (Fig. 8) correspond to the Lande factors $g_{eff,\ PB}$.

Table 1 – Some characteristics of selected spectral lines

No.	Element, multiplet	λ, Å	*EP*, eV	W_{ekv}, mÅ	$g_{eff,\ LS}$	$g_{eff,\ PB}$
1	Na I – 1 (D1)	5895.923	0.00	564	1.33	1.36
2	Na I – 1 (D2)	5889.953	0.00	752	0.75	1.22
3	He I – 1 (D3)	5875.6	20.87	-	-	0.94
4	Ni I – 68	5892.883	1.99	66	1.00	-
5	H I – 1(Hα)	6562.817	10.20	4020	1.05	1.00

The validity of using such factors for the D3 line follows from the calculations by Yakovkin and Lozitsky (2023), performed using the HAZEL code (Asensio Ramos et al., 2008). It was found that for magnetic fields with a strength of 500–2000 G, the Paschen-Back effect is already taking place in the D3 HeI line. As for the Hα line, the partial Paschen-Back effect occurs in it at the field strengths of ≈10 kG, and the complete Paschen-Back regime is reached when the magnetic fields approach 100 kG (Yakovkin and Lozitsky, 2022).

To reduce the noise effects in the line profiles, which are caused by the graininess of the photoemulsion in the spectrogram, the data were averaged twice: over spatial intervals equivalent to 1 Mm on the Sun, and over wavelength intervals of 50 mÅ, which corresponds to the width (namely, FWHM) of the instrumental profile of the Echelle spectrograph in of the diffraction order containing the D3 line.

The strongest emissions, which reached approximately 2–3 units of the nearest spectral continuum intensity level, were observed in the Hα and D3 lines, see Figs. 2 and 3. In these Figures, as well as Figs. 4–6, photometric profiles $I + V$ and $I - V$ are presented; the red curve represents the $I + V$ profiles, the blue $I - V$. The wavelengths were determined using telluric H_2O lines; the accuracy of such determination is approximately 2 mÅ.

As for the Hα line, its profiles in the flare are somewhat asymmetric, with a relatively weak "red" shift, and the central intensities in the $I + V$ and $I – V$ profiles almost matching. In contrast, such profiles for the D3 line are very different in intensity and have a noticeable relative shift in wavelengths, indicating a certain magnitude of the magnetic field. Both lines have a similar detail: a slight difference in the $I \pm V$ profiles in the far "blue" wings of the lines, at distances $\Delta\lambda \approx -3$ to -6 Å from the centers of the emission peaks, which indicates the presence of a weak circular polarization of one sign. No counterpart of the opposite polarity in the other wing of the emission ($\Delta\lambda > 0$) was found, contrary to the cases reported when analyzing other flares in Yakovkin and Lozitsky (2022, 2023).

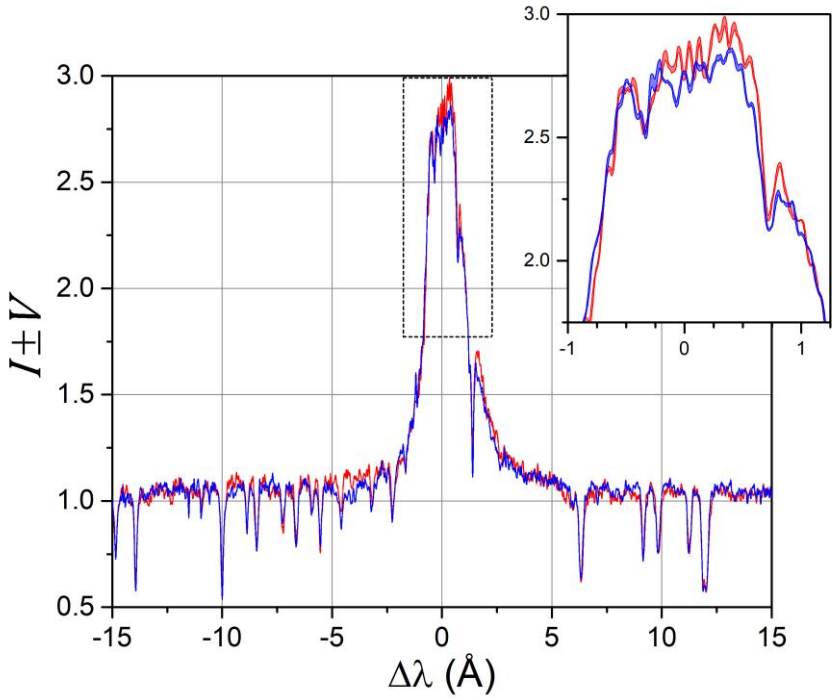

Figure 2. Observed $I \pm V$ profiles of the Hα line at the brightest point of the flare, corresponding to the distance along the slit L = 12 Mm. The inset shows the upper part of the profiles in an enlarged view, highlighting a weak relative displacement of the profiles which corresponds to a magnetic field of approximately 600 G.

The $I \pm V$ profiles in the spectral region containing the D2, Ni I 5892.883, and D1 lines are presented in Fig. 4. In this figure, in addition to the indicated solar lines, narrow telluric lines of molecular water are also visible, in particular, at $\lambda - \lambda_{D3}$ equal to 10.38, 11.62, and 12.06 Å. The D1 and D2 lines correspond to the $\lambda - \lambda_{D3}$ values of 20.32 Å and 14.32 Å, respectively, and the nickel line is located at $\lambda - \lambda_{D3} \approx 17.28$ Å. It can be seen that the emission in the chromospheric lines is relatively weak: it reaches a level of only ≈ 0.5 in the units of the adjacent spectral continuum intensity. In the same active region outside the flare, the central intensities of these lines were in the range of 0.06-0.09.

From Fig. 4, it can be seen that the nickel line shows no signs of significant splitting, which indicates a weak magnetic field at the level of its formation in the Sun's atmosphere if this magnetic field is considered to be purely longitudinal. Similarly, we see no noticeable splitting of the Fraunhofer absorption wings of D1 and D2 lines. However, an interesting situation is visible in the cores of these lines, where signs of a strong splitting of the emission peaks are

clearly visible, especially in the D1 line. The details of this splitting are presented in Figs. 5 and 6, where the thickness of the lines represents the 67% confidence interval.

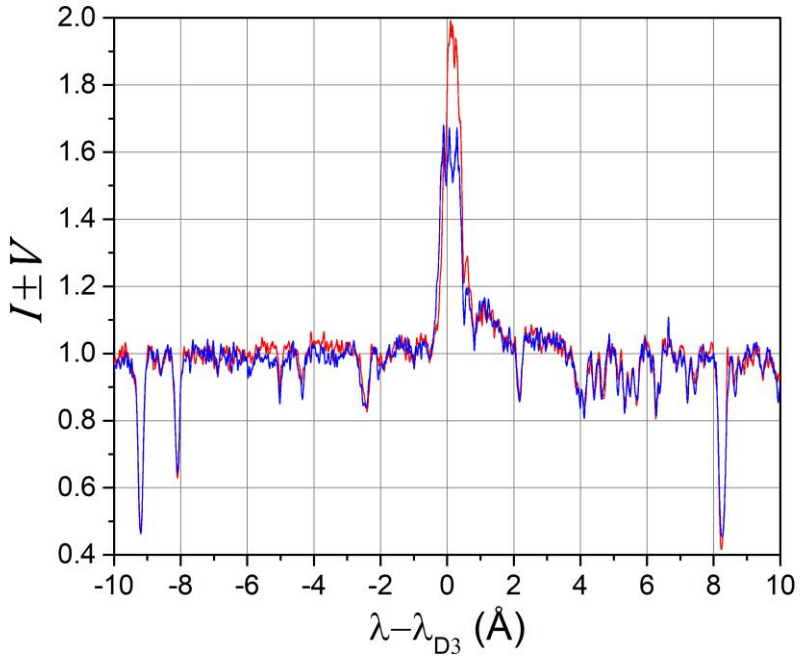

Figure 3. Observed $I \pm V$ profiles of the D3 line at L = 12 Mm. A significant difference in the amplitudes of the emission peaks in opposite circular polarizations is apparent, as well as a more noticeable compared to the case of Hα relative wavelength shift of the emission peaks. Such a shift corresponds to the magnetic field strength of 1.9 kG.

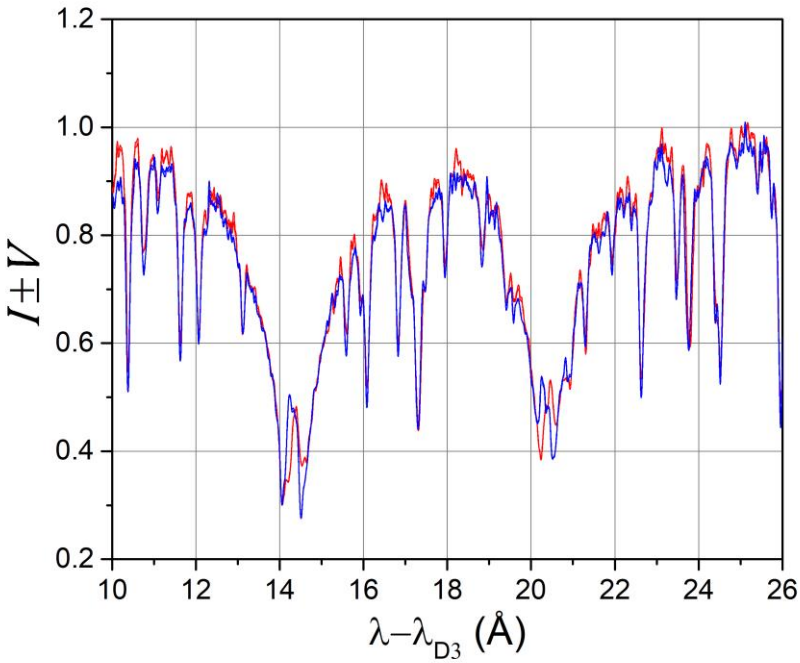

Figure 4. Observed $I \pm V$ profiles at L = 12 Mm within the spectral interval containing the D2, Ni I 5892.883 and D1 lines. The abscissa shows the wavelengths relative to the wavelength λ_{D3} of the D3 line.

The likely reason that the D1 line shows a sharper splitting of the emission peaks than the D2 line is the difference in the structure of their Zeeman sigma components. In the D1 line, the sigma components are singlet, with a 4/3 splitting factor when compared to the normal Lorentzian splitting, while in D2 these components are doublets – they consist of two subcomponents, with 3/3 and 5/3 splitting factors (Frisch, 2010). This results not only in different effective Lande factors, but also in a spectral broadening of the observed sigma components if the magnetic field is insufficient to completely separate these components.

3.2. Magnetic fields

For a more reliable measurement of magnetic field in the flare, only the steepest sections of the profiles of these lines, outside the intense blend lines, were taken into account. In these areas, the bisectors of the $I + V$ and $I - V$ profiles were calculated, and from their splitting $\Delta\lambda_b$, the Zeeman splitting $\Delta\lambda_H$ was estimated in the approximation of a purely longitudinal magnetic field, i.e. assuming that the splitting of the bisectors is equal to the doubled Zeeman splitting: $\Delta\lambda_b = 2\Delta\lambda_H$. It should be noted that this method of measuring Zeeman splitting is similar in nature to the classical magnetographic measurements (Babcock, 1953), in which the polarization signal is recorded at the steepest sections of the profiles (that is, at the peaks of $dI/d\lambda$), which ensures the maximum sensitivity of the measurements.

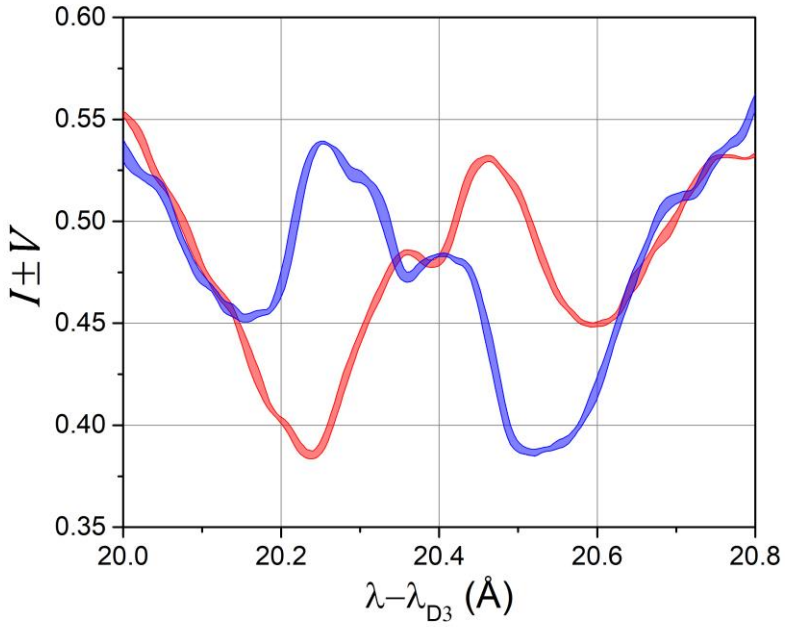

Figure 5. Observed $I \pm V$ profiles in the D1 line core near the location of the strongest flare emission corresponding to the distance along the slit L = 11 Mm. The splitting of the emission maximums corresponds to B = 4.8 kG.

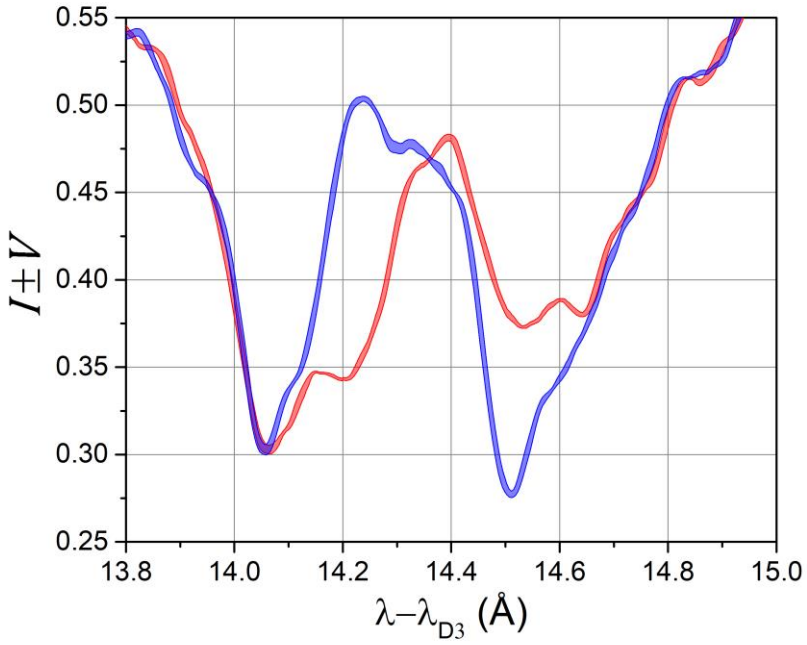

Figure 6. Observed $I \pm V$ profiles in the D2 line core at L = 11 Mm. The splitting of the emission maximums corresponds to B = 4.2 kG.

A well-known calibration formula was used to link the Zeeman splitting $\Delta\lambda_H$ to the magnetic strength B:

$$\Delta\lambda_H = 4.67\times10^{-13} g_{eff} \lambda^2 B = C\times10^{-5} B, \qquad (1)$$

where the magnetic splitting $\Delta\lambda_H$ and wavelength λ are expressed in angstroms (Å), and the magnetic field strength B – in gauss (G). The constant C, taking into account the effective Lande factors g_{eff} and wavelength λ according to the Table. 1, is the following for D1, D2, D3, H-alpha and Ni I 5892.88 Å lines: 2.20, 1.97, 1.51, 2.01 and 1.62, respectively.

We measured the magnetic fields by D1, D2 lines in the strong field approximation, SFA, and by the other lines in the weak field approximation, WFA. The differences between these approximations, and the contexts in which they are applicable are summarized below. In the weak-field approximation, the $I + V$ and $I - V$ profiles are close to Gaussian and unimodal, their relative splitting is small relative to their half-width (FWHM). In this case, the Stokes V parameter can be written as

$$V = C\,(dI/d\lambda)\,B_{LOS}, \qquad (2)$$

where C is the constant introduced above, $dI/d\lambda$ is the intensity gradient in the Stokes I profile, B_{LOS} is the longitudinal component of the magnetic field. From the given expression we have

$$B_{LOS} = V / C(dI/d\lambda). \qquad (3)$$

If the magnetic field is uniform, then the measured magnetic field strength does not depend on the distance from the center of the line. In other words, the bisectors (centroids) of the $I + V$ and $I - V$ profiles must be parallel to each other. In such a case, the results are insensitive to the exact method used for measuring the magnetic field: the measurement of the amplitudes of the V and ($dI/d\lambda$) parameters and the measurement of the relative displacement of the $I + V$ and $I - V$ profiles would give the same resulting magnetic field estimates.

In the strong field approximation, the $I + V$ and $I - V$ profiles have a different appearance: they deviate from Gaussian shapes, and a bimodal distribution of intensities becomes outlined or clearly manifested. This occurs when there is a central unshifted component (i.e., the Zeeman π component) and highly split side components, i.e., the Zeeman σ components. Consequently, it is quite logical and straightforward to measure the Zeeman splitting directly from the separation of the side σ components, where this splitting is equal to $2\Delta\lambda_H$. The existence of the strong field regime is also evidenced by the observed Stokes V profiles, which display an inflection point near the center of the line (Fig. 7 d). In the weak-field approximation, such an inflection point theoretically should not exist (Unno, 1956).

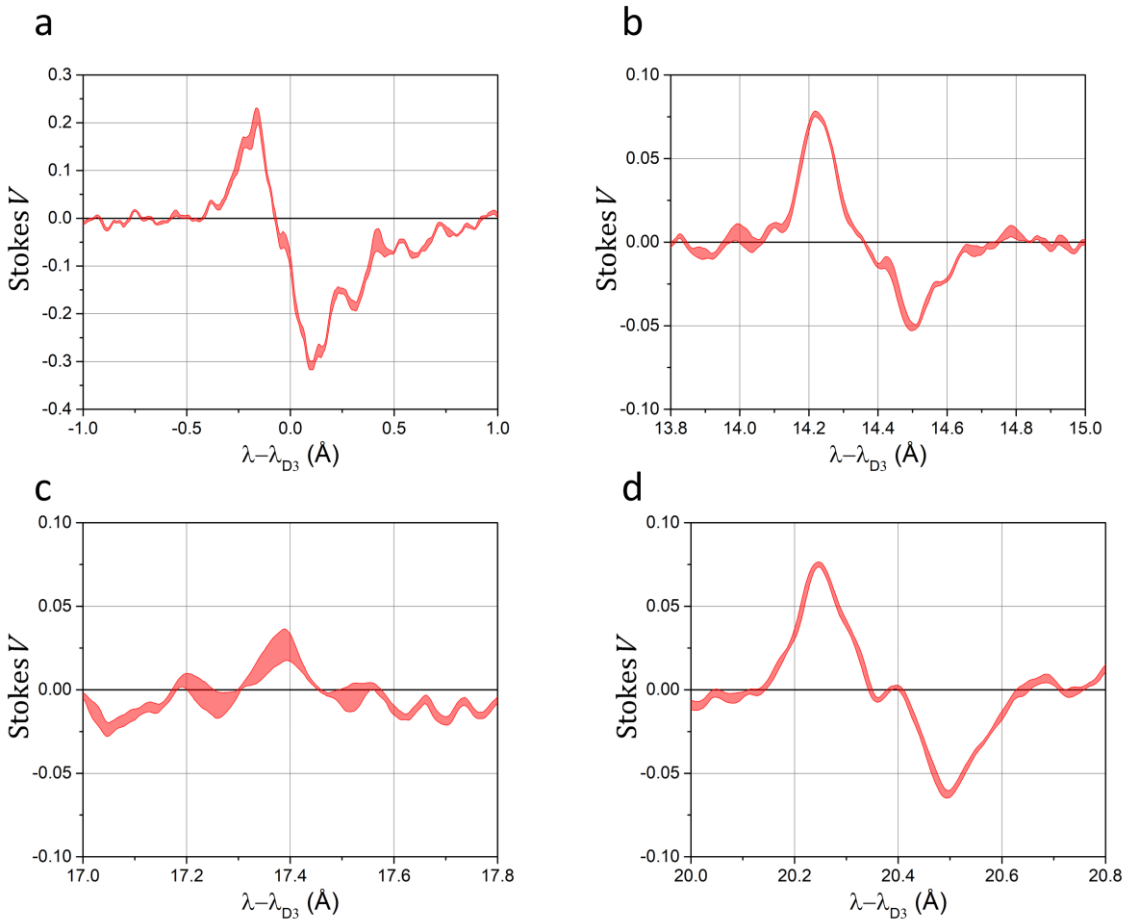

Figure 7. Comparison of the Stokes V profiles for L = 12 Mm of the D3 (a), D2 (b), Ni I 5892.88 Å (c), and D1 (d) lines. Thickness of the lines in the graph represents a 67% confidence interval.

Simply ignoring the signs of the strong-field regime and trying to use the weak-field approximation by comparing the amplitudes of V and $dI/d\lambda$ can quickly lead to incorrect conclusions regarding the magnetic field strengths. For example, the locations with non-zero V parameter and ($dI/d\lambda \rightarrow 0$) would suggest an infinite magnetic field strength, which is clearly not the case.

For the case presented in Fig. 7d, the corresponding comparative calculations were performed and it turned out that in the approximation of a strong field, the magnitude of the intensity is equal to approximately 6 kG, while in the weak field approximation it is ≈ 110 kG. The latter, as explained above, is a result of the fact that the parameter $dI/d\lambda \rightarrow 0$ in those places where the amplitude of the parameter V is maximum, that is, at the centers of the lateral sigma components. Figure 7c shows that the Ni I line showed no significant Stokes V polarization. This leads to the conclusion that the magnitude of the photospheric magnetic field below a solar flare (more precisely, its longitudinal component B_{LOS}) is also close to zero. The measured magnetic fields are summarized in Fig. 8.

One can see, that the maximum magnetic field strength in the flare reached 4.7–6.0 kG when measured by the D1 and D2 lines, 1.9 kG by the D3 line, and only 0.6 kG by the H-alpha and Ni I lines; typical errors of measurements are 0.1 kG.

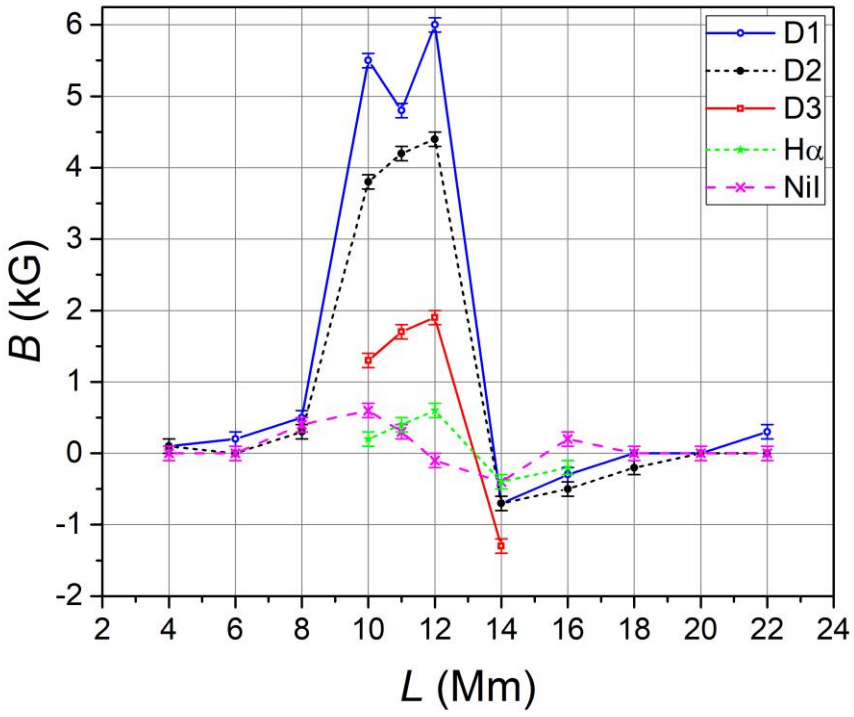

Figure 8. Comparison of magnetic field measurements using different spectral lines at different locations along the entrance slit of the Echelle spectrograph.

The high values of the magnetic field by D1 and D2 lines are quite understandable, since they correspond more closely to the strong field approximation, SFA. The data on the other lines correspond to the weak field mode, WFA, and reflect some effective field B_{eff}, which

corresponds to the longitudinal component $B_{LOS} = B_{\parallel}$ only when the filling factor f is equal to unity. If $f << 1$, then $B_{eff} \approx f B_{LOS}$ (Stenflo, 2011).

It is interesting that the D3 line at L = 12 Mm shows a much stronger magnetic field (1.9 kG) than the Hα line (0.6 kG), while the Ni I line shows an almost zero field at the same place. This shows the significant altitudinal heterogeneity of the magnetic field in the flare. The change of the magnetic field modulus with height (with its maximum in the chromosphere) is also evidenced by a comparison of the data by lines D1, D2 in the flare with the magnetic field in the sunspot closest to the flare, measured using Fe I 5250.2 line in the mode of full splitting of the Zeeman sigma components. According to the visual measurements of one of the authors of the paper (V.L.), the magnetic field in the spot was 2.8 kG, that is, significantly less than the 6 kG in the flare at the level of the chromosphere.

3.3. *Doppler velocities*

Doppler velocities were determined by the displacement of the studied lines relative to their undisturbed position in the spectrum as presented in Table 1. For this purpose, the wavelengths of the telluric and studied lines were compared on the registograms. The spectral displacement of the studied lines relative to their undisturbed position λ_0 was calibrated in velocities using the formula of Doppler's law $v = c(\Delta\lambda/\lambda_0)$ where c is the speed of light.

The general distribution of the Doppler velocities in the flare is quite complex, and the most interesting feature in it is that there were velocities of different signs at the same locations in the flare (Fig. 9).

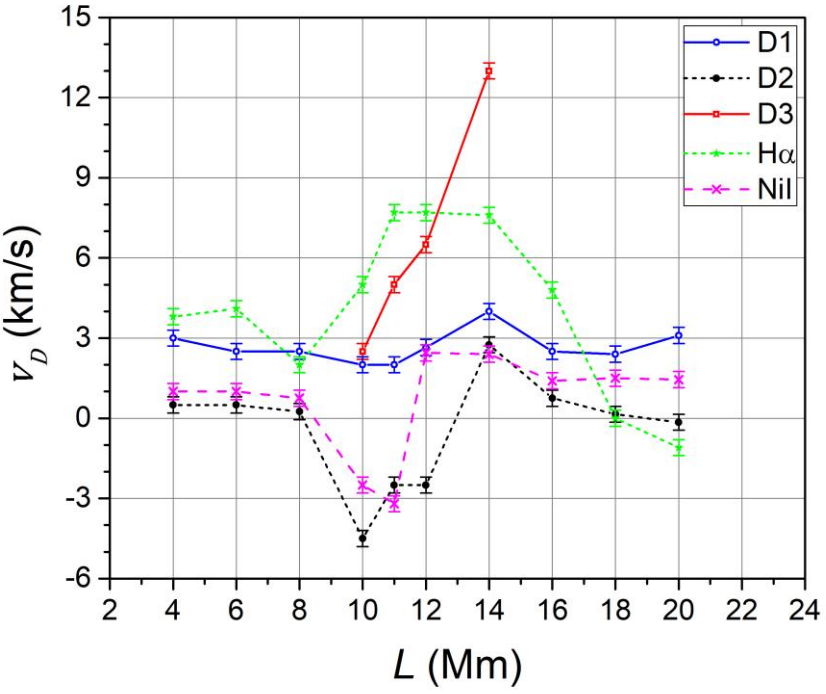

Figure 9. Comparison of Doppler velocities v_D by different spectral lines along the direction of the entrance slit of the spectrograph. The typical measurement error is 0.3 km/sec.

This means that in the flare there were counter movements of plasma, which, when the magnetic field is frozen in the substance, should lead to a local strengthening of the magnetic field at certain levels in the atmosphere. For example, at L = 12 Mm, the velocities of +2.65 km s^{-1} in the D1 line and -2.5 km s^{-1} in the D2 line were measured. This is especially interesting because one would expect very similar heights of formation of these lines in the solar atmosphere, because these sodium lines belong to the same multiplet, have the same excitation potential of the lower term and close equivalent widths in the spectrum of the quiet Sun (see Table 1 above).

Strictly speaking, plasma concentration increase and magnetic field amplification can take place even at velocities of the same sign. Indeed, Fig. 9 suggests that when moving from the upper level of the atmosphere (D3 and Hα lines) to the lower one (D1, D2 and Ni I lines), the velocities, in general, decrease in absolute value. This can mean that some of the energy released when the plasma slows down is spent on concentrating it to a higher density, as well as on strengthening the magnetic field.

The highest absolute velocities were measured by the D3 and H-alpha lines (7.5–13 km/s). This result is quite expected, taking into account that the area of formation of these lines refers to the upper chromosphere – the transition zone, that is, the closest, according to modern theory, to the area of the main energy release of the flare (Priest, 2014). From the comparison of Figs. 8 and 9, it can be seen that at $L \approx 11.5$ Mm, the sign of both the photospheric magnetic fields and the Doppler velocities indicated by the Ni I line changed. Such a close correlation is not observed in the chromospheric lines. Beyond the intense emission of the flare (for L = 4–8 and 18–20 Mm), both the velocities and the magnetic fields are much smaller in amplitude than in the flare, and their structure in different spectral lines is, in general, simpler.

It should be noted, that our velocity measurements may reflect the result of averaging sub-telescopic separated flows, including and streams of different signs. Given this, our data represent only a lower limit on the local velocities in the flare. However, even the lower speed limit is of interest in such a violent and powerful process on the Sun as a flare. In addition, since the altitudinal variations of the velocities reflect only the longitudinal component, the true pattern of the velocities may be more complex.

3.4. *Stokes V in wide spectral intervals*

In connection with the problem of the possible existence of extremely strong magnetic fields of 10^4–10^5 G range (Yakovkin and Lozitsky, 2022, 2023), it is of particular interest to study the Stokes V profiles in a wide range of wavelengths relative to the D3 and Hα lines. Fig. 10 presents the corresponding data for the flare under study in the range of wavelengths from –12.5 to +25 Å relative to the D3 line.

It can be seen from Fig. 10 that for the D3 line, the largest amplitude changes of both parameters take place within approximately ± 1 Å from the D3 line core. At the wavelengths λ–λ_D of +14.37 Å and +20.33 Å, even narrower peaks of both signs are observed, associated with the splitting of emission profiles of the D2 and D1 lines, respectively. The highlighted features represent the primary peaks of the Stokes V of the mentioned spectral lines.

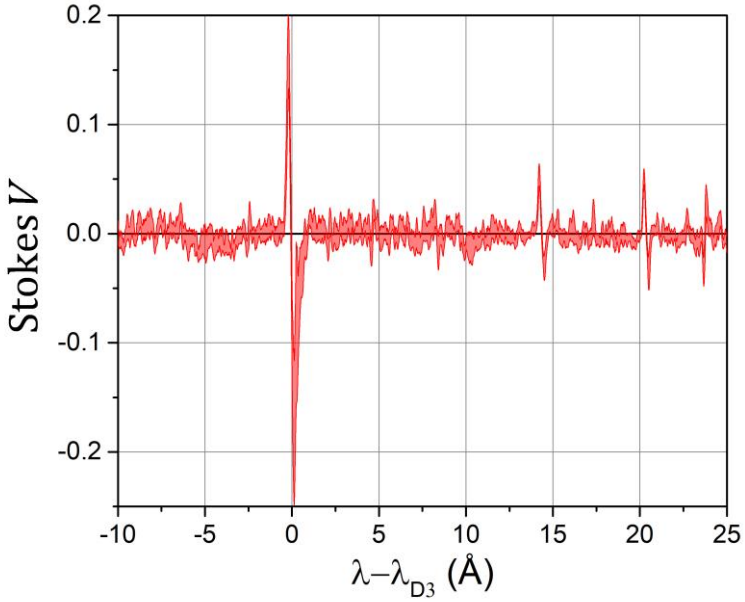

Figure 10. Observed Stokes *V* in range of wavelengths from -12.5 to + 25 Å relative to the D3 line averaged within the height interval of *L* = 10 – 12 Mm. The line thickness denotes the 67% confidence band.

As for the weaker secondary peaks, one can spot a hint of one-sign polarization at $\lambda–\lambda_D$ of –6...–3 Å. This is exactly the distance at which a weak difference between the $I + V$ and $I – V$ profiles can be seen in Figures 2 and 3, as in the Hα line, as well as in the D3 line. Such a feature is similar to the ones reported in Yakovkin and Lozitsky (2022, 2023), which were attributed to the presence of strong magnetic fields. However, when compared to the confidence band, we cannot state that the one-signed polarization at –6...–3 Å is statistically significant. Moreover, there is no counterpart of the opposite sign at $\lambda–\lambda_D$ of +3...+6 Å. Therefore, in this case, there is no reason to claim that we have spectral manifestations of particularly strong magnetic fields. It should be clarified that in recent works, in order to detect such characteristic features, a strong smoothing of the observed spectrum was carried out, with a smoothing window of about 0.3 Å, and such an averaged picture was also compared with the distribution of the $dI/d\lambda$ parameter, which represents the expected effect in the case of a weak field approach. However, a similar procedure was also carried out for the studied flare of 17 July 2004 and it did not reveal any reliable effects that could indicate particularly strong magnetic fields of 10^4–10^5 G range.

4. Discussion

The obtained data indicate a very complex altitudinal inhomogeneity of the magnetic field and radial velocities in the flare under study. From these data, a non-trivial situation emerges – a positive height gradient of the magnetic field in the flare, given that the photospheric line NiI 5892.883 Å shows a smaller measured field than the chromosphere lines D1 and D2, as well as D3 (Fig. 8). It is well known that in sunspots without flares, the altitudinal gradient of the magnetic field is negative (Solanki, 2003). Other studies also noted that in solar flares the

magnetic field at the upper level of the atmosphere is stronger than at the lower level (see, for example, Lozitskaya and Lozitskii (1982); Harvey (2012). Indeed, in these studies, the question remained open, whether this is really an increase in the magnetic field intensity magnitude with height, or the result of a complex interplay of many parameters. It should be emphasized that the mentioned measurements correspond to the weak-field regime, where the measured Zeeman splitting is much smaller than the spectral half-width (FWHM) of the line. In such a case, the results of the measurements probably reflect not only the local and background magnetic field strengths, but also the corresponding filling factors, magnetic polarities, angles of inclination of field lines, etc. Reliable data on the magnitude of the magnetic field in the region of solar flares can be obtained only in the strong field regime, when the Zeeman splitting is larger than the half-width of the spectral line. This requires data in spectrally narrow lines that have large Lande factors.

To the best of our knowledge, the first major results on the mentioned problem were obtained by Koval and Stepanyan (1972), who used direct spectral-polarization measurements in the CaI 6102.7 and FeI 6302.5 lines with Lande factors of 2.0 and 2.5, respectively. Observing the complete Zeeman splitting of these lines in sunspots that were closest to solar flares, these authors found that before the flare, the magnetic field strength at the upper level (i.e., in the CaI 6102.7 line) is 100–600 G higher than at the lower level (line FeI 6302.5). This difference persisted during flares, and after flares it changed to the opposite, when the magnetic field at the upper level was weaker than at the lower one.

It is possible that in solar flares there are local amplifications of not only magnetic fields, but also electric fields. The spectral effects of electric fields in the flare region were evaluated by Chen et al (2020) for the Hα line. As for the investigated flare of 17 July 2004, the electric fields in it can be indicated by the excess polarization at the tops of the emission peaks of the D3 line (Fig. 3), which is not typical for the Zeeman and Paschen – Back effects. Of course, it should be taken into account that the electric field does not create circular polarization, but only linear polarization, which can be registered only with a transverse field, that is, when the angle between the field vector and the line of sight is close to 90 degrees. However, at a certain level of instrumental polarization (when linear polarization is transformed into circular), a certain effect can also be detected with a circular polarization analyzer. This issue requires an additional separate study in the future works.

It should be noted that in the paper by Chen et al (2020), a different estimate of the magnetic field in the flare was obtained, namely 600 G, instead of 6 kG as indicated by the D1 line. However, it should be taken into account that that radio emission data 34 GHz and optical data in D1 and D2 sodium lines refer to different heights in the solar atmosphere. Radiation at a frequency of 34 GHz is formed in the transition zone between the chromosphere and the corona, while lines D1 and D2 are formed much lower – in the middle chromosphere (Vernazza et al., 1981.) If the magnetic field changes significantly with height in the atmosphere, then the magnetic field measurements will differ significantly between the 34 GHz and sodium lines. Therefore, we are inclined to the point of view that both estimates of magnetic fields (600 G and 6 kG) may be simultaneously correct, granted that they refer to different layers in the Sun's atmosphere. Notably, the Hα line has similar formation heights as the 3 GHz emission, and the corresponding magnetic field measurements therefore do match quite well: our results indicate

the magnetic fields ranging from –400 to +600 G depending on the location along the slit. It should also be noted that the used methodology involving the sodium lines corresponds to the one typically used for the sunspot magnetic field measurements. Such measurements are directly related to the atomic term structure and do not require additional model assumptions.

The detected difference in the Doppler velocities by D1 and D2 lines is also important from a methodological point of view, namely, for testing the possible use of these lines in the "line ratio" method (Stenflo, 1973) for diagnosing the spatially unresolved structure of the magnetic field in the chromosphere. For the photospheric level, the "line ratio" method was successfully applied due to the comparison of measurements in 2–3 selected FeI photospheric lines – those that belong to the same multiplet, have almost the same excitation potentials of the lower term and oscillator strength, but significantly different Lande factors (Stenflo, 1973; Wiehr, 1978; Cerdena et al., 2003). It was established by this method for the first time that magnetic fields in quiet regions on the Sun reach kilogauss values (1–2 kG), being concentrated in very thin (spatially unresolved) magnetic tubes called fluxtubes. This conclusion is obtained on the basis of two-component models, while assuming that the heights of the formations of the corresponding suitable lines are the same.

For the D1 and D2 lines, this assumption, as indicated above, cannot be applied. In fact, the formation heights of these lines are so different in the investigated flare that the corresponding Doppler velocities quite reliably do not match in magnitude (Fig. 9). Another obstacle to the very attractive task of using these lines to diagnose the sub-telescopic structure of the magnetic field in the chromosphere is that their Lande factors actually differ only a little due to the Paschen-Buck effect – only by ≈ 12%, see above Table 1. If their Lande factors corresponded to the *LS* coupling, then they would differ by a factor of 1.78, which would be quite valuable in the "line ratio" method.

5. Conclusion

The main conclusion of our work is that rather strong magnetic fields, about 6 kG, were registered at the chromospheric level of the solar flare by the D1 NaI line. It should be emphasized that these high values represent the modulus of the magnetic field strength, and not the longitudinal component, as in most measurements based on the Stokes V or $I \pm V$ profiles. A comparison of these measurements with similar measurements in other spectral lines (as well as in the Fe I 5250.2 line in the sunspot closest to the flare) suggests that these strong magnetic fields could have arisen directly in the chromosphere – as a result of the concentration of the magnetic field by countermovements of plasma, as indicated by the Doppler velocities in different spectral lines. As for the data on the effective magnetic field B_{eff}, which in the one-component magnetic field approximation should represent the longitudinal B_{LOS} component, the most interesting result is that the D3 line shows the strongest magnetic field compared to the Hα line and the photospheric Ni I line. It also indicates the concentration of the magnetic field in the area of the main energy release of the flare (its "collapse"). The highest Doppler velocities of plasma descent in the flare region are also measured in the D3 line.

Acknowledgements

The authors are grateful to unknown reviewers for their useful comments. This study was funded by Ministry of Education and Science of Ukraine (Kyiv, UA), project No. 22 БФ023–03.

Data availability

The original contribution presented in the study are included in the article.

References

Asensio Ramos A., Trujillo Bueno J., Landi Degl'Innocenti E., 2008. Advanced forward modeling and inversion of Stokes profiles resulting from the joint action of the Hanle and Zeeman effects. The Astrophysical Journal, 683, 542-565. https://doi.org/10.1086/589433

Babcock H. W., 1953. The solar magnetograph. Astrophysical Journal. 118, 387–396. https://articles.adsabs.harvard.edu/pdf/1953ApJ...118..387B

Banasek J. T., Engelbrecht J. T., Pikoz S. A., et al., 2003. Measuring 10-20 T magnetic fields in single wire explosions using Zeeman splitting. Review of Scientific Instruments. 87, 103506. https://doi.org/10.1063/1.4965836

Cerdena D., Almeida J. S., Kneer F., 2003. Inter-network magnetic fields observed with sub-arcsec resolution. Astronomy & Astrophysics. 407, 741–757. https://doi.org/10.1051/0004-6361:20030892

Chen B., Shen C., Gary D.E., et al., 2020. Measurement of magnetic field and relativistic electrons along a solar flare current sheet. Nature Astronomy. 4, 1140-1147.

Durán J. S. C., Lagg A., Solanki S. K., et al., 2020. Detection of the strongest magnetic field in a sunspot light bridge. The Astrophysical Journal. 895(2), 129–146. https://iopscience.iop.org/article/10.3847/1538-4357/ab83f1/meta

Frish S.E., 2010. Optical atom spectra. St.-Peterburg. Moscow. Krasnodar, 656 p.

Harvey J.W., 2012. Chromospheric magnetic field measurements in a flare and an active region filament. Solar Phys. 280, 69–81. https://doi.org/10.1007/s11207-012-0067-9

Hori H., Miki M., Date M., 1982. Pashen-Back effect in D-lines sodium under a high magnetic field. Journal of the Physical Society of Japan. 51(5), 1566–1570. https://doi.org/10.1143/JPSJ.51.1566

Kleint L., 2017. First detection of chromospheric magnetic field changes during an X1-flare. Astrophysical Journal. 834, art. id. 26, 10 pp. https://doi.org/10.3847/1538-4357/834/1/26

Koval A. N., Stepanyan N. N., 1972. Changes in the magnetic fields of sunspots at two levels in connection with the development of active regions. Solnechnyje Dannyje. 1, 83-91 (in Russian).

Libbrecht T., de la Cruz Rodriguez J., Danilovic S., et al., 2019. Chromospheric condensations and magnetic field in a C3.6-class flare studied via He I D3 spectro-polarimetry. Astronomy & Astrophysics. 621, id.A35, 21 pp. https://doi.org/10.1051/0004-6361/201833610

Livingston W., Harvey J. W., Malanushenko O. V., et al., 2006. Sunspots with the strongest magnetic fields. Solar Physics. 239, 41-68. https://doi.org/10.1007/s11207-006-0265-4

Lozitska N. I., Lozitsky V. G., Andryeyeva O. A., et al., 2015. Methodical problems of magnetic field measurements in umbra of sunspots. Advances in Space Research. 55(3), 897–907. https://doi.org/1016/j.asr.2014.08.006

Lozitska N. I., Yakovkin I. I., Lozitsky V. G., 2024. Unique spectral manifestations around the D3 line observed in the region close to the seismic source of a large solar flare. Monthly

Notices of the Royal Astronomical Society: Letters. 528, L1–L3. https://doi.org/10.1093/mnrasl/slad163

Lozitskaya, N. I., Lozitskii V. G., 1982. Do "magnetic transients" exist in solar flares? Soviet Astronomy Letters. 8, 270-272. https://www.osti.gov/biblio/5988127

Lozitsky V. G., 2016. Indications of 8-kilogauss magnetic field existence in the sunspot umbra. Advances in Space Research. 57, 398–407. . https://doi.org/10.1016/j.asr.2015.08.032

Lozitsky V., Yurchyshyn V., Ahn K., et al., 2022. Observations of extremely strong magnetic fields in active region NOAA 12673 using GST magnetic field measurement. The Astrophysical Journal. 928 (1), id.41, 7 pp. https://doi.org/10.3847/1538-4357/ac5518

Moore Ch. E., Minnaert, M. G. J., Houtgast J. (1966). The solar spectrum 2935 Å to 8770 Å. *National Bureau of Standards, Washington: US Government Printing Office (USGPO)*. https://articles.adsabs.harvard.edu/pdf/1966sst..book.....M

Parker E. N., 2001. Solar activity and classical physics. Chinese Journal on Astronomy and Astrophysics. 1, 99–124. https://doi.org/10.1088/1009-9271/1/2/99

Pevtsov, A. A., Bertello L., Tlatov A. G., Kilcik A., et al., 2014. Cyclic and Long-Term Variation of Sunspot Magnetic Fields. Solar Phys., 289 (2), 593–602. https://doi.org/10.1007/s11207-012-0220-5

Priest E. R., 2014. Magnetohydrodynamics of the Sun. Cambridge University Press. https://doi.org/10.1017/CBO9781139020732

Quintero Noda C., Schlichenmaier R., Bellot Rubio L. R. et al., 2022. The European Solar Telescope. Astronomy and Astrophysics. 666. A21. https://doi.org/10.1051/0004-6361/202243867

Scherrer P. H., Bogart R. S., Bush R. I. et al., 1995. The solar oscillations investigation – Michelson Doppler Imager. Solar Physics. 162, 129–188. https://doi.org/10.1007/BF00733429

Solanki S. K., 2003. Sunspots: An overview. Astronomy and Astrophysics Review. 11, 153–286. doi:10.1007/s00159-003-0018-4

Stenflo J. O., 1973. Magnetic-field structure of the photospheric network. Solar Physics. 32, 41–63. https://doi.org/10.1007/BF00152728

Stenflo J. O., 1985. LEST – a Large International Solar Telescope for the 1990'S / Large European Solar Telescope. Vistas in Astronomy. 28, 571–576. https://doi.org/10.1016/0083-6656(85)90078-9

Stenflo, J. O., 2011. Collapsed, uncollapsed, and hidden magnetic flux on the quiet Sun. Astronomy and Astrophysics. 529, id.A42, 20. https://doi.org/10.1051/0004-6361/201016275

Unno W., 1956. Line formation of a normal Zeeman triplet. Publications of Astronomical Society of Japan. 8, 108–125. https://articles.adsabs.harvard.edu/full/1956PASJ....8..108U

Vernazza J. E., Avrett E. H., Loeser R., 1981. Structure of the solar chromosphere. II. Models of the EUV brightness components of the quiet-sun. Astrophysical Journal Supplement Series. 45, 635-725. https://doi.org/10.1086/190731

Wiehr E., 1978. A unique magnetic field range for non-spot solar magnetic regions. Astronomy and Astrophysics. 69(2), 279–284. https://articles.adsabs.harvard.edu/pdf/1978A%26A....69..279W

Yakovkin I. I., Lozitsky V. G., 2022. Signatures of superstrong magnetic fields in a limb solar flare from observations of the Hα line. Advances in Space Research. 69. 4408-4418. https://doi.org/10.1016/j.asr.2022.04.012

Yakovkin I. I., Lozitsky V. G., 2023, Search for superstrong magnetic fields in active processes on the Sun using spectro-polarimetry within 15 angstroms around the D3 line. Monthly

Notices of the Royal Astronomical Society. 523, 5812–5822, https://doi.org/10.1093/mnras/stad1816